Hexatic and mesoscopic phases in the 2D quantum Coulomb system

Bryan K. Clark,[1] Michele Casula,[2] and D. M. Ceperley[1,3]
[1] *Department of Physics, University of Illinois at Urbana-Champaign, 1110 W. Green St, Urbana, IL 61801, USA*
[2] *Centre de Physique Théorique, Ecole Polytechnique, CNRS, 91128 Palaiseau, France*
[3] *NCSA, University of Illinois at Urbana-Champaign, Urbana, IL 61801, USA*
(Dated: May 27, 2009)

We study the Wigner crystal melting in a two dimensional quantum system of particles interacting via the $1/r$ Coulomb potential. We use quantum Monte Carlo methods to calculate its phase diagram, locate the Wigner crystal region, and analyze its instabilities towards the liquid phase. We discuss the role of quantum effects in the critical behavior of the system, and compare our numerical results with the classical theory of melting, and the microemulsion theory of frustrated Coulomb systems. We find a Pomeranchuk effect much larger then in solid helium. In addition, we find that the exponent for the algebraic decay of the hexatic phase differs significantly from the Kosterilitz-Thouless theory of melting. We search for the existence of mesoscopic phases and find evidence of metastable bubbles but no mesoscopic phase that is stable in equilibrium.

PACS numbers: 29.25.Bx. 41.75.-i, 41.75.Lx

The Wigner crystal (WC) melting has been a subject of intense study over the years.[1, 2, 3] A better understanding of this process is particularly important in the two dimensional (2D) one component plasma (OCP) with $1/r$ Coulomb interactions, since it could explain many features in systems such as electrons at interfaces, dusty plasmas, MOSFETs, and charged colloids.

Although in 2D, a true crystalline order is not possible at any finite temperature T [4], a quasi-long range translational order is stable at strong coupling. Upon melting from the WC a variety of mechanisms have been proposed.[1] At high temperature, Halperin and Nelson [5] suggested that the 2D melting is a two-step process, with a hexatic phase in between. Hexatic phases have been seen in colloids, liquid crystals, and dusty plasmas,[6] and found in some classical simulations.[7, 8] However, there is disagreement about its location, critical exponents, and order. The influence of quantum effects is unclear.

In the ground state, Jamei *et al.* [9] argue by a mean-field approach that a first order WC-liquid transition at zero temperature is disallowed; instead the transition is mediated by microemulsion phases (e.g. stripes or bubbles). This mechanism might be related to the stripe order in some strongly correlated materials and anomalous effects in experiments on MOSFETs.[10]

In this Letter, we examine a 2D system of N quantum distinguishable (Boltzmannon) particles that interact with a Hamiltonian:

$$H = -\frac{1}{r_s^2}\sum_i \nabla_i^2 + \sum_{i<j}\frac{2}{r_s|\mathbf{r}_i - \mathbf{r}_j|} + V_{\rm bg}, \qquad (1)$$

where $\mathbf{r}_i$ is the location of the i'th particle. The system is parameterized by two dimensionless parameters which we choose to be r_s and T. We use $a = r_s a_0$ as the unit of length, with a_0 the Bohr radius, Rydberg as the unit of energy, and temperature; the density is $1/\pi(r_s a_0)^2$. The system is neutralized by a rigid homogeneous background, which gives rise to the constant $V_{\rm bg}$. Our goal is to map out the phase diagram, to locate the WC phase boundaries, and analyze the transition to the liquid. To do so, we use quantum Monte Carlo (QMC) techniques, which are uniquely suited for calculations of the properties of strongly coupled Coulomb systems.

At finite temperature, we use path integral Monte Carlo (PIMC),[11] to sample configurations from the thermal density matrix. In contrast to fermion systems, for a system of distinguishable particles, there is no sign problem. All systematic errors, such as the time step and finite size errors, can be studied with extrapolation. [22] Our calculations involve approximately 100 phase points at system ranging from 200 to 2248 particles and between 10 and 8000 slices in imaginary time.

At $T = 0$, we use diffusion Monte Carlo (DMC), a projector method that takes as input a trial wave function Ψ_T, and filters from it, all excited states. Calculating DMC energies in this system is formally exact as long as Ψ_T has a non-zero overlap with the ground state.

General properties of the phase diagram - Our proposed phase diagram is shown in Fig. 1. The boundary between the WC and the liquid phase presents a clear re-entrant behavior at low T. Although such behavior has been seen in helium,[14, 15] for the 2D-OCP the effect is significantly stronger. We find the ratio between the minimal and maximal density of the crystal 0.6 compared to 0.03 for He^3 and $3\cdot10^{-5}$ for He^4. The re-entrant liquid terminates in a zero temperature quantum critical point (QCP) at $r_s \simeq 66.5 \pm 0.2$. This differs by 10 % from previous DMC simulations;[12] our calculations did a more careful extrapolation to the thermodynamic limit.[13]

At large r_s we compare our results with simulations done for the classical OCP; classical simulations found a WC phase stable for $\Gamma > 140$ and a liquid phase stable for $\Gamma < 120$,[8] where $\Gamma = 2/r_s T$. Seen as lines in Fig. 1, these values compare favorably with our results at large

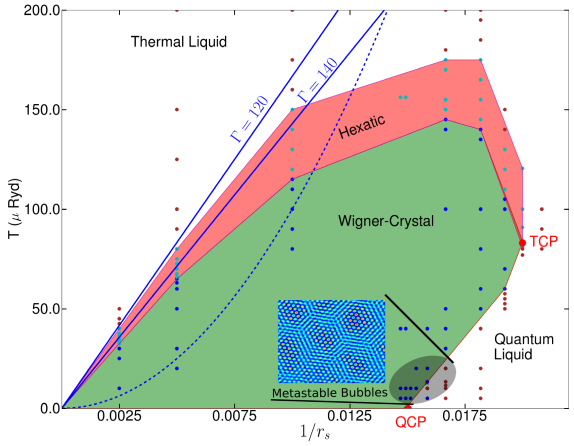

FIG. 1: Phase diagram of the quantum 2D Coulomb system calculated using QMC as obtained by analyzing correlation functions. Points indicate location of QMC calculations. The phase boundaries are interpolations between these points. The dotted blue line indicates a rough separation between the classical and the quantum regions: when the thermal de Broglie wave length equals the interparticle spacing. The solid straight blue lines are the classical results of Ref. [8]. The inset is a density profile of the metastable bubbles seen in PIMC.

r_s. For $120 \leq \Gamma \leq 140$, we found a hexatic quasi-long range order; this order extends into the quantum regime by bending with respect to the classical line as the density is increased (i.e. for $r_s < 200$).

At $r_s \simeq 60$ the melting temperature decreases until it reaches a tricritical point (TCP), located at $r_s \simeq 50$ and $T \simeq 80$ μRyd, where the isotropic liquid, the hexatic phase, and the WC coexist. We have used the Clausius-Clapeyron relation to understand this behavior. For Coulomb systems it reads[16]:

$$\frac{dT}{d(1/r_s)} = \frac{2}{\Gamma}\frac{\delta K + \delta U}{\delta U}, \qquad (2)$$

where $\delta U = U_c - U_h$ and $\delta K = K_c - K_h$ are the changes in the internal and kinetic energies between the crystal (U_c, K_c) and hexatic (U_h, K_h) phase. The slope is shown in Fig. 2. At the downturn, the slope is zero, while it diverges at the TCP, where the entropy difference, and hence δU, goes to zero. In fact, Eq. 2 shows that a first order line for any Coulomb system, must become second order at the nose of a re-entrant phase.

There are two WC-to-liquid boundaries: the quantum melting line, going from the QCP to the TCP, and the thermal melting line, flowing from the high temperature side of the TCP towards lower density (large r_s), and characterized by a two-step process mediated by a hexatic phase. The order of the phase transitions is established by examining the internal energy per particle $U = U(T)$ at a series of densities $r_s \in (48, 400)$ through

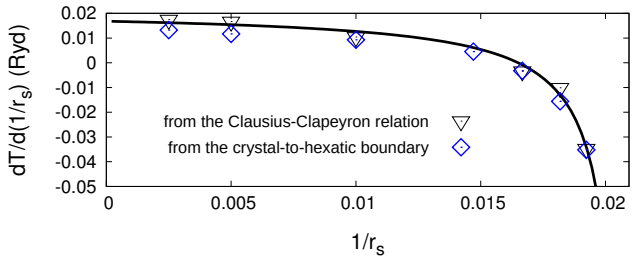

FIG. 2: $dT/d(1/r_s)$ vs $1/r_s$ computed using the Clausius-Clapeyron relation, Eq. 2 for $N = 562$, compared with the results obtained directly from the phase diagram in Fig. 1 for the first order WC-to-hexatic boundary.

a wide range of temperatures. The behavior at $r_s = 55$ is shown in Fig. 3. A second order (or weakly first order) phase transition is evident for the quantum melting line, indicated by a kink in the internal energy when moving from the re-entrant liquid phase to the WC. Increasing the temperature, $U(T)$ shows a sharp jump at the boundary between the solid and hexatic phase, indicating a first order WC-hexatic transition. The internal energy is continuous between the hexatic phase and the liquid, indicating a continuous hexatic-liquid transition. This is in disagreement with the classical theory of melting, which suggests two continuous transitions of Kosterlitz-Thouless (KT) type. It should be noted that as one approaches the classical limit, r_s (≈ 400), the jump in energy shrinks and becomes barely distinguishable from a continuous transition.

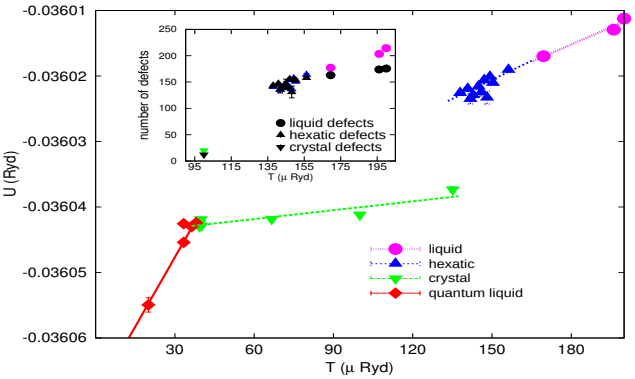

FIG. 3: Internal energy per particle versus temperature at $r_s = 55$ for $N = 562$. The inset plots both the number of defects and the internal energy scaled to arbitrary units and shifted.

Thermal melting line - The thermal melting line is characterized by the presence of a hexatic intermediate phase with an order parameter:

$$g_6(r) = \left\langle \sum_{ij} \Psi^*(\mathbf{r}_i)\Psi(\mathbf{r}_j)\delta((|\mathbf{r}_i - \mathbf{r}_j|) - r) \right\rangle, \qquad (3)$$

where $\Psi(\mathbf{r}_i) = \frac{1}{6}\sum_{\langle j\rangle} \exp(6i\theta_{ij})$; the summation is over nearest neighbor particles j surrounding i, [23] and θ_{ij} is the angle between an arbitrary fixed vector and the vector joining $\mathbf{r}_i$ to $\mathbf{r}_j$. The algebraic decay of $g_6(r)$ signals a quasi-long range orientational order and this, combined with a lack of translational order, defines the hexatic phase. Additionally, the orientational order of the hexatic phase manifests itself via a sixfold anisotropy in the structure factor $S(\mathbf{k})$. Fig. 4 shows the behavior of the $S(\mathbf{k})$ in the liquid, solid, and hexatic phases at $r_s = 55$, and $g_6(r)$ as a function of temperature. There is a clear qualitative change in the decay of $g_6(r)$ for $156.2\ \mu Ryd \leq T \leq 150.3\ \mu Ryd$, as we transition from the liquid to the hexatic phase.

The KT theory predicts that for hexatic systems in the XY universality class $g_6(r) \propto r^{-\eta_6}$, with $\eta_6 \leq 1/4$, and η_6 reaching its maximum $1/4$ at the transition to the liquid. We fit the large distance values of $g_6(r)$, to determine η_6 and found that, independent of temperature, it undergoes the hexatic-to-liquid transition for $\eta_6 \simeq 2$. The disagreement with the KT theory is likely due to the $1/r$ interaction. Indeed, critical exponents in other models, for example the Ising model, are known to be strongly affected by the range of the interaction.[17]

Defects play an important role in 2D melting. We define defects using a Voronoi construction of each particle's centroid. In a perfect hexagonal lattice, each centroid has six neighbors. Defective centroids, say with 5 or 7 neighbors, are denoted as vortices and antivortices respectively. According to the KT theory the WC-hexatic transition is caused by the unbinding of dislocations (particles defined as strongly bound vortex-antivortex pair), while the hexatic-liquid transition is driven by the vortex-antivortex unbinding. However, important differences are found in our system. At the verge of the WC melting, instead of the expected continuous rise of dislocations, the number of defects jumps discontinuously. We see a strong correlation between the energy and the number of defects; $U(T)$ in the hexatic and solid phases is controlled entirely by their number. Therefore, the first order jump seen in $U(T)$ at the WC-hexatic transition is due to the proliferation of dislocations in the system, which can be induced by grain boundaries,[18, 19] present in the WC phase. The inset of Fig. 3 shows this proportionality by plotting both the defect number and the energy of the various phases on the same axis, with the $U(T)$ scaled to arbitrary units and shifted. We note that the first order transition in a long range system is unconventional because the presence of the background does not allow macroscopic separation of phases with different densities. In the hexatic-liquid transition, the number of defects grows slowly while the energy of the system rises at a much faster rate suggesting the presence of an unbinding process possibly related to the vortex-antivortex melting.[5]

Quantum melting line - The quantum melting line goes from the QCP to the TCP. Jamei *et al.*[9] and Ortix *et al.*[20] showed recently by a mean-field Hamiltonian that the system undergoes a WC-liquid transition at $T = 0$ through a sequence of intermediate phases such as stripes, or other "microemulsion phases". Their shape and size depend on the parameters of the mean-field Hamiltonian. At the critical density r_s^c, where the free energy of the crystal equals that of the liquid, the optimal geometry is found to be alternating liquid and crystal stripes of width $W_0 = a\exp(\lambda)$, with a a lattice cutoff proportional to the mean interparticle spac-

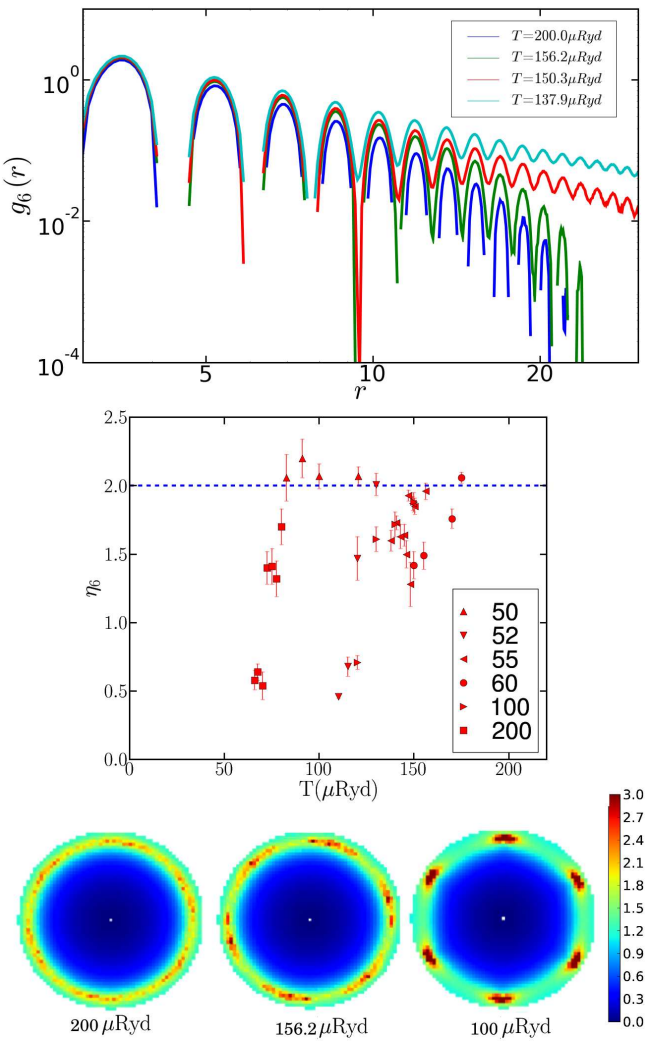

FIG. 4: Top: $g_6(r)$ at different temperatures for $r_s = 55$, $N = 2248$. The lower two temperatures show algebraic decay while the higher temperatures decay faster than algebraically. Middle: $\eta_6(T)$ in the hexatic phase for $N = 562$ at various temperatures and densities (for r_s values, see legend on figure). All exponents satisfy $\eta_6 \lesssim 2$ (shown as dotted line). Bottom: $S(\mathbf{k_x}, \mathbf{k_y})$ in a liquid, hexatic, and solid respectively for $r_s = 55$, $N = 562$, temperatures in caption.

ing, $\lambda = 4\pi^2 e^2 \sigma / \Delta\mu_c^2$, where σ the surface tension, and $\Delta\mu_c = \mu_{\rm crys}(r_s^c) - \mu_{\rm liq}(r_s^c)$ the chemical potential difference between the crystal and liquid at criticality.

At finite T, our PIMC results suggest a second order (or very weakly first order) direct transition. We carefully searched for mesoscopic phases in the surrounding region. At $r_s \approx 55$, where the transition temperature to the re-entrant liquid is relatively high ($T \simeq 50\ \mu Ryd$), we find no evidence for mesoscopic phases. At larger r_s and, hence, lower transition temperature, the PIMC simulations occasionally yield inhomogenous phases. A density profile of such a phase is shown in the inset of Fig. 1. However, those inhomogenous structures appear to be metastable because their internal energy, measured in PIMC at low T ($< 10\ \mu Ryd$) and DMC at T=0, is always higher than the homogenous phases. To clarify this situation, we performed additional DMC simulations to determine the parameters of the mean-field model. In the liquid phase, we used a pair product or Jastrow trial function $\Psi_{\rm liquid} = \prod_{i<j} \exp[-u_{RPA}(|\mathbf{r}_i - \mathbf{r}_j|)]$, with u_{RPA} the RPA Jastrow function.[21] For the solid and stripe phase we multiplied by a Gaussian, tieing the distinguishable particles to predefined sites, $\{\mathbf{I}_i\}$ arranged to correspond to a crystal or stripe: $\Psi_{\rm crystal} = \Psi_{\rm liquid} \exp[-\sum_i \alpha |\mathbf{r}_i - \mathbf{I}_i|^2]$. We fit the $T = 0$ liquid and crystal energies to a polynomial and, assuming the transition is weakly first order, obtain $r_s^c = 66.5 \pm 0.2$ and $\Delta\mu_c = 65 \pm 5\ \mu Ryd$.

We estimate the surface tension σ by computing the energy at r_s^c for different number of stripes,[24] and hence different surface length in the system: $\sigma_{\rm stripe} = 1.55 \pm 0.09\ \mu Ryd/a_0$. Plugging $\sigma_{\rm stripe}$ and $\Delta\mu_c$ in the equation for λ gives $\lambda \approx 3 \times 10^5$, which leads to the width of the stripes at the critical point of $W_0 \approx 10^{10^5}$: much larger than any physical system. The large widths are a result of very small difference in the chemical potential between the homogeneous liquid and crystal phases at the QCP, characteristic of the $1/r$ interaction. Away from r_s^c, the periodicity of the alternating stripes will become even larger. Therefore, the instability towards "microemulsion phases" has a characteristic emergent length W_0 so large that it cannot explain non-Fermi liquid behavior seen in 2D experimental setups.[10]

Conclusion - We have studied the WC melting in the 2D quantum Coulomb system of particles with Boltzmann statistics. Its phase diagram shows thermal and quantum melting. The thermal melting is mediated by a hexatic phase, but significant deviations from the classical KT theory are found. The WC-hexatic transition is first order, driven by the proliferations of defects in the crystal, where they are assembled into grain boundaries. The hexatic parameter $\eta_6 \approx 2$ belongs to the universality class of long-range models and reveals the importance of the long-range interaction in determining the transition properties. In the low temperature region, we found a strong Pomeranchuck effect, much larger than for solid helium. At low temperatures, we did not find stable microemulsion phases. An estimate of their size is exceedingly large, which makes this kind of phases impossible to see in any physical system if driven by correlation effects only.

We acknowledge support from NSF grant DMR-0404853 and EAR 05-30643. MC also thanks the Centre de Physique Théorique of the Ecole Polytechnique. Supercomputer calculations were done at the NCSA. We would also like to thank also Frank Kruger for his careful reading and John A. Goree and Yu. E. Lozovik for useful discussions.

[1] K. J. Strandburg, Rev. Mod. Phys. **60**, 161 (1988).
[2] K. Wierschem and E. Manousakis, Int. J. Mod. Phys. B **20** (19), 2667 (2006).
[3] C. Mora, O. Parcollet, and X. Waintal, Phys. Rev. B **76**, 064511 (2007).
[4] B. Jancovici, Phys. Rev. B **19**, 20 (1967).
[5] D. R. Nelson, and B. I. Halperin, Phys. Rev. B **19**, 2457 (1979).
[6] R. A. Quinn and J. Goree, Phys. Rev. E **64**, 051404 (2001); H. H. von Grünberg, P. Keim, K. Zahn, and G. Maret, Phys. Rev. Lett. **93**, 255703 (2004); X. H. Zheng and R. Grieve, Phys. Rev. B **73**, 064205 (2006).
[7] W. J. He, T. Cui, Y. M. Ma, Z. M. Liu, and G. T. Zou, Phys. Rev. B **68**, 195104 (2003).
[8] S. Muto, and H. Aoki, Phys. Rev. B **59**, 14911(1999).
[9] R. Jamei, S. Kivelson, and B. Spivak, Phys. Rev. Lett. **94**, 056805 (2005).
[10] E. Abrahams, S. V. Kravchenko, and M. P. Sarachik, Rev. Mod. Phys. **73**, 251 (2001).
[11] D. M. Ceperley, Rev. Mod. Phys. **67**, 279 (1995).
[12] S. De Palo, S. Conti, and S. Moroni, Phys. Rev. B **69**, 035109 (2004).
[13] S. Chiesa, D. M. Ceperley, R. M. Martin, and Markus Holzmann, Phys. Rev. Lett. **97**, 076404 (2006).
[14] I. Pomeranchuk, Zh. Eksp. Teor. Fiz. **20**, 919 (1950).
[15] L. Goldstein, Phys. Rev. Lett **5**, 104 (1960).
[16] M. D. Jones and D. M. Ceperley, Phys. Rev. Lett **76**, 4572 (1996).
[17] E. Luijten, and H. W. J. Blöte, Phys. Rev. Lett **89**, 025703 (2002).
[18] D. S. Fisher, B. I. Halperin, R. Morf, Phys. Rev. B **20**, 4692 (1979).
[19] S. T. Chui, Phys. Rev. B **28**, 178 (1983).
[20] C. Ortix, J. Lorenzana, M. Beccaria, and C. Di Castro, Phys. Rev. B **75**, 195107 (2007).
[21] D. M. Ceperley, Phys. Rev. B **18**, 3126 (1978).
[22] Most of the path integral calculations were done using the pair action approximation of the diagonal and with a time step $\tau = 50$. A study of time step error indicates that the forms of the phases as well as differences in energy have converged.
[23] Nearest neighbors to i are all particles j with $|\mathbf{r}_i - \mathbf{r}_j| < 2.54$.
[24] We exploit the small overlap between the liquid and the crystal wave function to project out the lowest energy in the Hilbert space within the same "phase" of the trial

function.